International Journal of Pharmaceutics 692 (2026) 126647

Contents lists available at ScienceDirect

International Journal of Pharmaceutics

journal homepage: www.elsevier.com/locate/ijpharm

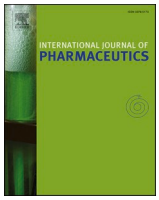

Indirect effects of pH on drug solubility in fed state simulated intestinal fluids

Mare Oja [a], Sepanta Ehtemam [a], Hristina Mircheva [b], Brecht Goovaerts [a], Patrick Augustijns [a], Zahari Vinarov [b,*]

[a] Drug Delivery and Disposition, Department of Pharmaceutical and Pharmacological Sciences, KU Leuven, Leuven, Belgium
[b] Department of Chemical and Pharmaceutical Engineering, Faculty of Chemistry and Pharmacy, Sofia University, Sofia, Bulgaria

ARTICLE INFO

Keywords:
Solubilization
Lipid
Micelles
Oleate
Partitioning
Colloids
Apparent solubility

ABSTRACT

The pH-mediated effect of drug ionization on solubility is well-described. However, pH can also indirectly influence solubility by altering the colloidal structures in human intestinal fluids. This study investigates the indirect pH effect on the apparent solubility of 13 uncharged drugs across a pH range of 4.5 to 7.5 in fed-state simulated intestinal fluids (SIF) composed of taurocholate and lecithin, with or without added lipids (monoolein and/or sodium oleate). A pronounced indirect pH effect on drug solubility was observed when oleate was present in the SIF, whereas monoolein had only a minor effect. Below pH 6.5, sodium oleate was converted to oleic acid, resulting in lipid droplet formation that enhanced lipophilic compound solubility in the total sample (lipid phase + micellar phase), while the micellar solubility remained similar to the reference SIF (without oleate). This resulted in an up to 50-fold increase of the ratio total/micellar drug solubility, which correlated well with drug lipophilicity or its combination with total polar surface area ($R^2 \approx 0.8$). At higher pH, a lipid phase was not formed because the ionized sodium oleate partitioned in the micellar phase, where it significantly increased drug solubilization. These findings highlight the importance of considering indirect pH effects in solubility assessments by tuning simulated intestinal fluids composition to better reflect *in vivo* reality.

1. Introduction

Drug solubility is a critical factor in oral drug absorption and bioavailability, which can be influenced by pH through two distinct mechanisms. The well-known direct pH effect on solubility involves ionization of the drug molecule characterized by its dissociation constant (pK_a) (Avdeef, 2007) and is a primary consideration in formulation development. In contrast, the indirect pH effect, which is related to the pH-dependent changes in colloidal structures (Suys et al., 2017), remains less understood despite its potential significance in complex biological environments such as human intestinal fluids (HIF).

HIF includes bile salts, phospholipids, proteins, cholesterol, and lipids (Vinarov et al., 2021), which can self-assemble into various colloidal structures, including micelles and lipid droplets (Riethorst et al., 2016a). These structures are highly sensitive to pH, which varies significantly depending on food and time (Riethorst et al., 2016b). Such pH fluctuations can alter the composition and behavior of colloidal assemblies (Suys et al., 2017), thereby influencing the apparent solubility of drugs (Vinarov et al., 2018). Among these components, lipids play a critical role. Depending on the pH, long chain fatty acids generated during lipid digestion or ingested as additives can exist in ionized or non-ionized forms ($pH \leq 6.5$), forming micelles, larger colloidal aggregates or a separate lipid phase (Salentinig et al., 2010; Suga et al., 2016). The pK_a of oleic and other long- and medium-chain fatty acids is higher than the reported $pK_a \approx 4.8$ of the soluble short-chain carboxylic acids, due to the formation of colloidal structures with highly charged surfaces which alter local pH and thus impact pK_a (Cistola et al., 1988). Previous studies have shown that in a complex dispersion such as HIF, the lipid distribution between the isotropic micellar phase and the lipid phase may depend on pH (Goovaerts et al., 2024). In the same publication, it has been shown that the lipid concentration in the micellar phase and total sample (the latter containing both lipid and micellar phases) is one of the parameters strongly affecting the apparent solubility of poorly water-soluble drugs in HIF.

* Corresponding author at: Department of Chemical and Pharmaceutical Engineering, Faculty of Chemistry and Pharmacy, Sofia University "St. Kl. Ohridski", 1 James Bourchier ave., 1164 Sofia, Bulgaria.
E-mail address: zv@lcpe.uni-sofia.bg (Z. Vinarov).

https://doi.org/10.1016/j.ijpharm.2026.126647
Received 12 November 2025; Received in revised form 28 January 2026; Accepted 31 January 2026
Available online 7 February 2026

Lipid concentration in duodenal HIF is significantly higher in the fed state compared to the fasted states. In the fasted state, reported values range from <1 mg/mL (Goovaerts et al., 2024) to 5.5 mg/mL (Clarysse et al., 2009). In the fed state, concentrations show greater variability, with values ranging from 7.3 to 14.9 mg/mL (Clarysse et al., 2009; de Waal et al., 2023; Goovaerts et al., 2024; Vinarov et al., 2021). This variability raises important questions about the extent to which the indirect pH effect influences drug apparent solubility under fed-state conditions, where lipid content is substantially higher and thus colloidal complexity is increased.

As obtaining HIF is time- and resource-consuming, simulated intestinal fluids (SIF) provide a controlled and reproducible system for investigating pH-dependent apparent solubility effects. Among commercially available fed-state SIFs, FeSSIF lacks lipids, while FeSSIF-V2 contains 0.80 mM (≈0.24 mg/ml) sodium oleate and 5.00 mM (1.78 mg/ml) glyceryl monooleate (Bou-Chacra et al., 2017). However, concentrations of free fatty acids in these media are markedly lower, while the levels of monooleate are notably higher than those found in average HIF under fed conditions (de Waal et al., 2023; Goovaerts et al., 2024). A lower concentration of sodium oleate in FeSSIF-V2 media was selected to obtain a single-phase system that is easier to prepare (Jantratid et al., 2008). Studies utilizing the design of experiments approach scanned different concentrations of sodium oleate and revealed a pH-effect for uncharged drug substances, suggesting a possible indication for indirect pH effect caused by the changes of colloidal structures (Dunn et al., 2019; Khadra et al., 2015). However, the assumption that neutral drugs do not have pH dependence had led to exclusion of pH as an influencing factor when the indirect pH effects were weak (Madsen et al., 2018).

The present study aims to systematically investigate the impact of the indirect pH effect on the apparent solubility of neutral drugs. pH-solubility profiles were measured for 13 uncharged drugs in four SIF media with low and high lipid content, across a physiologically relevant pH range (4.5–7.5). Both micellar phase and total sample (including lipid and micellar phase) were analyzed to capture the full extent of solubilization. By this approach, we comprehensively assessed how pH-driven colloidal transformations influence drug solubility in modified SIF.

2. Materials and methods

2.1. Chemicals

The model drugs were selected based on their physicochemical properties and low solubility. As the study aims to measure only the indirect pH effect, the selected 13 drugs were uncharged across the analyzed pH range (pH 4.5–7.5). The physicochemical characteristics of all model drugs are summarized in Table 1.

Sodium hydroxide and ritonavir were purchased from Sigma-Aldrich (St. Louis, MO). Sodium chloride, sodium acetate trihydrate and maleic acid were purchased from VWR International bvba (Leuven, Belgium). Hydrochloric acid, acetonitrile (AcN, HPLC grade) and mitotane were purchased from Fischer Scientific (Waltham, MA, USA) and methanol (MeOH, HPLC grade), dimethylsulfoxide, spironolactone and olaparib from Acros Organics (Geel, Belgium). Glacial acetic acid was bought from Chem-Lab NV (Zedelgem, Belgium). Griseofulvin was provided by Certa (Braine-l'Alleud, Belgium), and sorafenib and apixaban were acquired from Tebu bio. Merck Life Science B.V. (Hoeilaart, Belgium) provided fenofibrate, danazol, griseofulvin, and ritonavir. Loviride and etravirine were kindly provided by Johnson & Johnson Innovative Medicine (Beerse, Belgium). FaSSIF/FeSSIF/FaSSGF and FeSSIF-V2 powder to prepare fed state SIF was purchased from Biorelevant.com (Croydon, UK). Sodium oleate, celecoxib, and bicalutamide were purchased from TCI EUROPE N.V. (Zwijndrecht, Belgium). A penicillin and streptomycin mixture (PENStrep, 10,000 U/mL) was used to protect the media against bacterial growth and was provided by Lonza (Basel, Switzerland). Purified water was produced using a Purelab Flex water system from Veolia (Paris, France). All substances used for solubility experiments had purity above 95 %.

2.2. Simulated intestinal fluids

All SIF media were prepared using the original FeSSIF-V2 buffer formulation containing 55.02 mM maleic acid, 125.50 mM sodium chloride and 81.65 mM sodium hydroxide. The buffer pH was adjusted to 5.8 with 1 M sodium hydroxide or 1 M hydrochloric acid solution. pH measurements were performed using a SlimTrode pH electrode (Hamilton, VWR) and a Knick Portamess 911 pH meter (Berlin, Germany).

Two baseline SIF media were prepared using the maleic acid buffer. The FeSSIF medium was modified to match the bile salt concentration (10 mM) found in FeSSIF-V2 and this modified medium is referred to as FeSSIF* throughout the article. FeSSIF* was prepared by dissolving 74.6 mg FaSSIF/FeSSIF/FaSSGF powder (final concentration 7.46 mg/mL) in a 10.00 mL solution including 9.90 mL maleic acid buffer and 0.10 mL penicillin and streptomycin mixture (final activity of 100 U/mL), which was added to prevent bacterial degradation. The FeSSIF-V2 medium was prepared by dissolving 97.6 mg FeSSIF-V2 powder (final concentration 9.76 mg/mL) in a 10.00 mL solution, which included 9.90 mL maleic acid buffer and 0.10 mL penicillin and streptomycin mixture (final activity of 100 U/mL). The final concentrations of the components in each medium are summarized in Table 2.

Both media were mixed and equilibrated for two hours at room temperature prior to use. The pH of the obtained solution was 5.8. The pH of the baseline media was further fixed using 1 M NaOH and 1 M HCl solutions to four different pH values: pH 4.5, 5.5, 6.5, and 7.5,

Table 1
Physicochemical properties of the 13 model drugs.

Compound	MW (g/mol)	HB donors	HB acceptors	$logP_{ow}$	TPSA (Å^2)	pK_a	Melting point (°C)
Apixaban	459.5	1	5	2.2	111		326.53
Bicalutamide	430.4	2	9	2.3	116	12.0	192
Celecoxib	381.4	1	7	3.4	86.4	11.1	158
Danazol	337.5	1	3	3.8	46.3		
Etravirine	435.3	2	7	4.5	121	<3 (Schöller-Gyüre et al., 2009)	260 (Weuts et al., 2011)
Fenofibrate	360.8	0	4	5.2	52.6		80.5
Griseofulvin	352.8	0	6	2.2	71.1		220
Loviride	351.2	2	3	4.4	72.2		226.9 (Van Eerdenbrugh et al., 2007)
Mitotane	320.0	0	0	6.2	0		77
Olaparib	434.5	1	5	1.9	82.1		198
Ritonavir	720.9	4	9	6.0	203	1.8, 2.6 (Velozo et al., 2022)	122 (Bauer et al., 2001)
Sorafenib	464.8	3	7	4.1	92.4		205.6
Spironolactone	416.6	0	5	2.9	86.7		134.5

Most of the data presented in this table are sourced from PubChem (Kim et al., 2025). Entries with alternative sources are explicitly indicated.
MW: molecular weight; HB: hydrogen bond; $logP_{ow}$: logarithm of octanol–water partition coefficient, which was calculated using the XlogP3 3.0 method; TPSA: Topological polar surface area.

Table 2
Composition of the used SIF media.

	FeSSIF*	FeSSIF-V2	FeSSIF*+SO	FeSSIF-V2 + SO
From biorelevant powder				
Bile salt (taurocholate) (mM)	10.00	10.00	10.00	10.00
Phospholipid (lecithin) (mM)	2.5	2.00	2.5	2.00
Glyceryl monooleate (mM)		5.00		5.00
Sodium oleate (mM)		0.80		0.80
Additionally added				
Sodium oleate (mM)			42.48	42.48

corresponding to the range of reported pH values in duodenum HIF (Harder et al., 2025; Riethorst et al., 2016b).

Two more complex media, FeSSIF*+SO and FeSSIF-V2 + SO (Table 2), were prepared by adding 129.3 mg sodium oleate (SO, final concentration 12.93 mg/mL) to 10 mL of the respective baseline media (FeSSIF* and FeSSIF-V2). Sodium oleate was added to mimic the lipid phase found in HIF (Goovaerts et al., 2024; Riethorst et al., 2018), which is absent in the reference SIF. Sodium oleate was selected as the sole lipid component, as 91 % of the lipids measured in HIF were fatty acids and the digested liquid meal was composed of 88 % unsaturated fats (Goovaerts et al., 2024). As we approximated the total lipid composition in fed state HIF to a single fatty acid, its concentration was also selected to correspond to the total lipid concentration measured in the same study. Hence, the total lipids in HIF (12 mg/mL, Goovaerts et al., 2024) were taken as oleic acid, which are equivalent to the 12.93 mg/mL sodium oleate used in the current study. Sodium oleate was used instead of oleic acid as sodium oleate dissolves faster and adjusts the natural pH of the media from 5.8 to ≈ 7 during sample preparation, preventing the formation of a lipid phase that could stick to the glassware.

The homogenous solution with pH ≈ 7 was used to pipette seven aliquots, from which we prepared seven media with pH values 4.5, 5.0, 5.5, 6.0, 6.5, 7.0, and 7.5, corresponding to previously reported pH values in duodenum HIF (Harder et al., 2025; Riethorst et al., 2016b). The pH was adjusted as described for the FeSSIF* and FeSSIF-V2 media.

2.3. Determination of apparent solubility of model compounds

2.3.1. Solubility method

The apparent equilibrium solubility of 13 drugs was determined in four SIF media (section 2.2). For solubility measurement, an excess amount of drug powder was added to a 0.5 mL Eppendorf tube, depending on the solubility of each drug. Approximately 0.30 ± 0.03 mg of powder was used for most drugs, resulting in a drug content of 1 mg/mL. Exceptions were made for drugs with higher solubility in total samples, such as ritonavir and fenofibrate, where 0.60 ± 0.06 mg of powder was used, resulting in a drug content of 2 mg/mL.

Special safety considerations were applied for anticancer drugs, including mitotane, sorafenib, olaparib, and bicalutamide, to minimize processing time during weighing. For mitotane, a powder range of 0.6–0.9 mg was allowed (drug content of 2–3 mg/mL), while for the other three anticancer drugs, the range was 0.3–0.6 mg (drug content of 1–2 mg/mL).

At the start of the solubility experiment, 300 μL of SIF was added to the pre-weighted drug powder in Eppendorf tubes. The resulting mixture was vortexed to create a suspension. The suspension was shaken at 175 rpm and 37 °C for 24 h (IKA KS 4000i control, Staufen, Germany). The shaking duration was chosen based on preliminary time dependence measurement (data not shown), demonstrating that equilibrium solubility for all drugs was achieved within 24 h in FeSSIF*+SO media at pH 5.8.

2.3.2. Sample treatment protocols

We determined two types of solubilities, which correspond to different compositions of the analyzed samples: total and micellar solubility. The total solubility reflects the sum of the concentrations of free drug (molecularly dissolved in the aqueous phase), drug solubilized in colloidal structures (micelles, vesicles, nanodroplets) and drug dissolved in the lipid phase (larger lipid droplets). The micellar solubility includes the free drug and the drug solubilized within colloidal structures (Vertzoni et al., 2022). Although only the free drug is believed to be directly available for absorption, colloidal structures can act as a reservoir, replenishing the free drug after its absorption (Fagerberg and Bergström, 2015). Hence, the solubilized drug can also have a significant influence on drug absorption.

For the reference media, FeSSIF* and FeSSIF-V2 (Table 2), drug solubility was determined in the micellar phase only, as these media remained homogeneous within the studied pH range and lipid phase was not present. The complex media, FeSSIF*+SO and FeSSIF-V2 + SO (Table 2), were turbid and inhomogeneous at low pH, hence their solubilizing capacity was assessed both in the total sample and in the micellar phase. Solubility values were determined in triplicate to ensure accuracy. The samples for determination of total and micellar solubility were obtained as described in the following subsections.

(A) Micellar sample preparation

First, all samples were centrifuged at 20817 × g and 37 °C for 30 min (Centrifuge 5804 R, Eppendorf, Hamburg, Germany). After centrifugation, a clear supernatant (the micellar phase) and a pellet (undissolved drug) were formed for FeSSIF* and FeSSIF-V2 samples. For samples prepared with FeSSIF*+SO and FeSSIF-V2 + SO media, centrifugation resulted in the formation of up to three layers: a solid pellet, a clear supernatant and a lipid layer on top (depending on pH). The formation of the lipid layer was pH-dependent, being more prominent at acidic pH values and absent at neutral pH values.

After centrifugation of the reference FeSSIF* and FeSSIF-V2 samples, the upper part of the sample was carefully removed using a suction system. Although a lipid layer was not present in these samples, the upper part was removed to avoid any contamination from incompletely wetted undissolved drug particles. An aliquot for solubility determination was taken from the middle part of the solution (avoiding contact with the tube walls and the solid part of the drug at the bottom). The collected samples were diluted in a 50:50 MeOH:H_2O mixture for HPLC analysis.

For samples prepared with FeSSIF*+SO and FeSSIF-V2 + SO media, the micellar phase was isolated by removing the upper lipid layer using a suction system. As the lipid layer can be disturbed during the suction (contaminating the micellar phase), approximately 130 μL of the micellar phase, free of solid particles, was transferred to a new tube. The transferred solution was vortexed and centrifuged again at 20,817 g and 37 °C for 30 min. After the second centrifugation, the lipid layer (if present) was removed using a suction system. A sample of micellar phase was taken and diluted in a 50:50 MeOH:H_2O mixture for HPLC analysis.

(B) Total sample preparation

To determine the total drug solubility in samples based on FeSSIF*+SO and FeSSIF-V2 + SO media (which both contained a lipid phase), they were first centrifuged at 20817 × g and 37 °C for 30 min. The liquid phase was then transferred to a new tube to eliminate the pellet of undissolved drug particles. During the transfer, visible lipid droplets were first moved to the new tube, then the upper layer was gently mixed to detach any lipid droplets that may have adhered to the plastic, and finally the rest of the liquid sample was transferred to the new tube. The transferred sample was homogenized using a vortex to ensure thorough mixing. The homogenized total sample was then diluted in a 50:50 MeOH:H_2O mixture (Table 3) for HPLC analyses.

Table 3
Sample preparation and HPLC parameters for model drugs.

Compound	Dilution of micellar and total samples in 50:50 MeOH: H_2O	Mobile phase	Flow rate (mL/min)	UV detection wavelength
Danazol	1:100 (v/v)	85:15 MeOH/ buffer	1.0	288 nm
Loviride	1:20 (v/v)	60:40 AcN/ buffer	1.0	366 nm
Fenofibrate	1:100 (v/v)	85:15 MeOH/ buffer	1.5	287 nm
Ritonavir	1:50 (v/v)	85:15 MeOH/ buffer	1.0	250 nm
Griseofulvin	1:100 (v/v)	70:30 MeOH/ buffer	1.0	298 nm
Etravirine	1:50 (v/v)	85:15 MeOH/ buffer	1.0	312 nm
Celecoxib	1:100 (v/v)	80:20 MeOH/ buffer	1.0	230 nm
Spironolactone	1:100 (v/v)	50:50 AcN/ buffer	1.0	237 nm
Bicalutamide	1:50 (v/v)	60:40 AcN/ buffer	1.0	280 nm
Mitotane	1:200 (v/v)	85:15 MeOH/ buffer	1.5	225 nm
Sorafenib	1:50 (v/v)	70:30 AcN/ buffer	1.0	265 nm
Olaparib	1:100 (v/v)	60:40 MeOH/ buffer	1.0	220 nm
Apixaban	1:20 (v/v)	40:60 AcN/ buffer	1.0	276 nm

2.3.3. HPLC analyses

The diluted samples were analyzed using an isocratic method on an HPLC system consisting of a Chromaster 5160 pump, 5260 Autosampler, and 5410 UV detector (VWR International). The HPLC parameters specific to each drug are shown in Table 3. The mobile phase buffer was a 25 mM acetic acid buffer at pH 4.5 for all drugs. The injection volume was 50 μL. The HPLC methods for all compounds were validated for accuracy, precision, and recovery following the FDA Bioanalytical Method Validation Guidance for Industry (Bioanalytical Method Validation Guidance for Industry | FDA, 2018). All HPLC methods for the compounds met the specified criteria.

2.4. Complex SIF media characterization

2.4.1. Lipid analysis

The total lipids in the micellar phase were determined in the FeSSIF*+SO and FeSSIF-V2 + SO media at a pH range of 4.5–7.5 to determine the distribution of lipids between the lipid and micellar phases. The concentrations of free fatty acids (FFAs), monoacylglycerides (MAGs), diacylglycerides (DAGs), and triglycerides (TAGs) were determined with high-performance liquid chromatography (HPLC) coupled to a charged aerosol detector (CAD) (Thermo Fisher Scientific, Waltham, MA). Only the sum of FFAs, MAGs, DAGs, and TAGs (i.e., total lipids) is reported, without specification of individual lipid classes. The detailed description of the analytical method is provided elsewhere (Goovaerts et al., 2024).

2.4.2. Size and zeta potential of colloidal structures

The size distribution and surface charge of colloidal particles in the oleate-supplemented SIF media were characterized using a Zetasizer Nano ZS (Malvern Instruments, UK) equipped with a 633 nm laser and a detection angle of 173°. Measurements were performed at 37 °C. Three consecutive measurements were performed for each sample, and the results were reported as the mean ± standard deviation.

For DLS, the hydrodynamic diameter (Z-average) and volume distribution were analyzed to evaluate the size and uniformity of colloidal aggregates. Zeta potential was measured using a high concentration zeta cell (Malvern Instruments, UK) and electrophoretic light scattering in order to assess the changes of the surface charge across the pH range of 4.5–7.5.

2.4.3. Microscope imaging

To visualize the microscopic morphology of the samples, they were imaged via polarized light microscopy. The samples were kept at a constant temperature of 37 °C, using a thermostatic cell on the microscope. To prepare the samples, a drop of the material was placed on a microscope slide, between two cover glasses, used as spacers. A third cover glass was placed on top to facilitate spreading of the sample and to minimize evaporation. Observations were performed using a Zeiss Axio Imager.M2m microscope (Germany) in transmitted, cross-polarized white light. A special λ-compensator plate was added between the sample and the analyzer, set at a 45° angle to both the polarizer and analyzer creating a magenta background in the images and helping highlight structural details.

3. Results and discussion

3.1. Characterization of oleate supplemented SIF

The FeSSIF*+SO and FeSSIF-V2 + SO media were characterized by analyzing changes in lipid content, surface charge, and size of colloidal structures across the studied range of pH values to reveal the impact of pH on the phase composition of the media and on the properties of the colloids.

3.1.1. Microscopic characterization

Visual observations during the preparation of the SIF samples showed dramatic changes in the appearance of all samples containing sodium oleate as a function of pH: the turbid dispersions obtained at low pH = 4.5 gradually transformed to completely clear solutions at neutral pH = 7.5. To gain more information on their morphology, both the total samples and micellar phases were imaged via polarized light microscopy.

The obtained images of the total samples clearly showed that an emulsion was formed at low pH = 4.5: lipid droplets were found in both FeSSIF*+SO and FeSSIF-V2 + SO media (Fig. 1). The droplet size distribution appeared bimodal, with one population of droplets with a diameter around 1 μm and a second population of much larger droplets, ranging in size from 5 to 30 μm. In addition, a grainy structure could be observed in several samples, which indicated the presence of nanodroplets that were beyond the resolution of an optical microscope.

Increasing the pH of the total samples gradually decreased the lipid droplet concentration and size and at pH = 6.0 only few, very small droplets could be visualized by the microscope (Fig. 1). At pH ≥ 6.5, the microscope images were clear, consistent with the clear appearance of the solutions, for both FeSSIF*+SO and FeSSIF-V2 + SO media (Supplementary Fig. S1).

The obtained results could be rationalized by considering the ionization behavior of oleic acid, which has a $pK_a \approx 6$ when solubilized in micellar structures (Salentinig et al., 2010). At low pH the oleate salt is converted to oleic acid, which forms a separate lipid phase (the observed emulsion droplets). Increasing the pH gradually transforms oleic acid back to oleate which has much higher solubility and surfactant-like

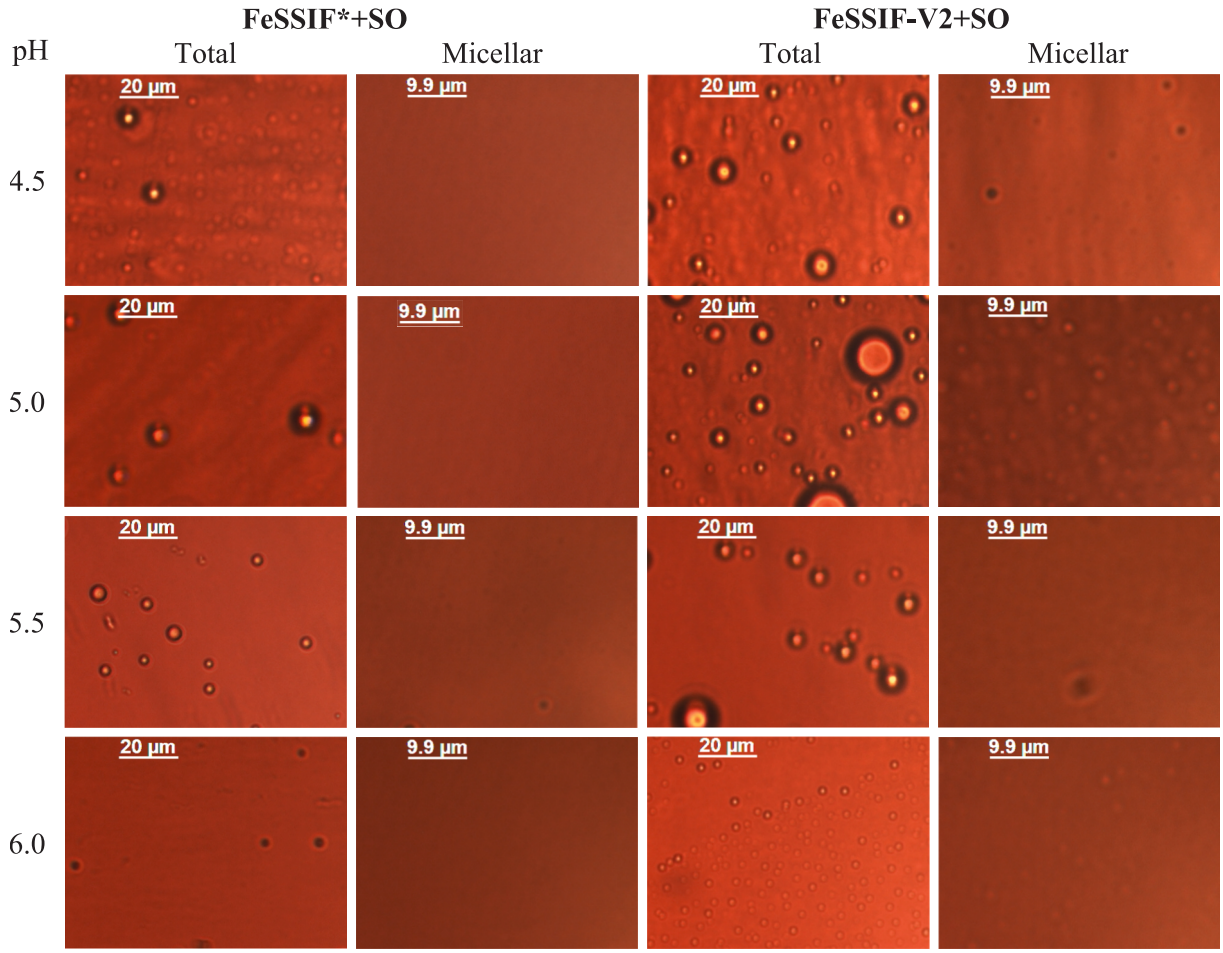

Fig. 1. Colloidal structures in total and micellar samples imaged in FeSSIF* + SO and FeSSIF-V2 + SO media at pH 4.5 to 6. The larger colloidal structures were identified in the total sample (first and third columns) and the colloidal structures were significantly smaller in the micellar sample (second and fourth columns).

behavior, triggering the formation of mixed micelles with the bile salts and phospholipids of the FeSSIF*+SO or and FeSSIF-V2 + SO media. As a result, the lipid droplet concentration and size decrease until the transformation is complete and all lipid droplets have disappeared.

After analyzing the total samples to clarify the phase behavior and morphology of the SIF, we then studied the extent to which the used sample treatment (centrifugation), performed under conditions commonly used for solubility assessment, could efficiently remove the lipid phase from the total sample. The main performance indicator was the lack of lipid droplets in the micellar phase, which was obtained after the sample treatment protocol.

In the FeSSIF*+SO media, the results showed single, very small lipid droplets in the micellar phase (Fig. 1), indicating that the majority of the lipid phase was successfully removed. In the case of FeSSIF-V2 + SO, a few small droplets were also observed, however, the grainy structure observed in the total samples was preserved at pH = 4.5 and 5.0. Hence, the sample treatment protocol successfully removed the majority of the lipid phase. To further investigate the properties of the micellar phase,

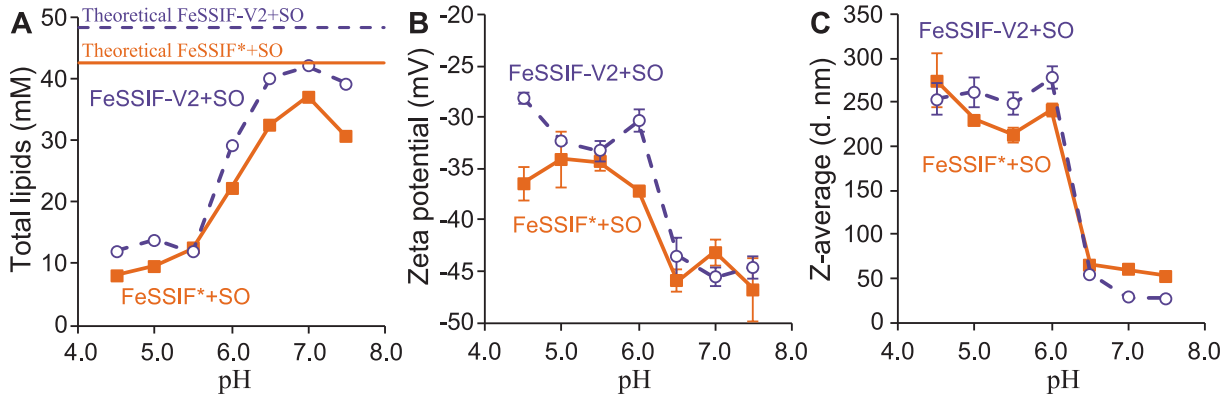

Fig. 2. pH profiles of total lipids concentration (n = 1, A), zeta potential (n = 3, B), and average diameter of colloidal particles (n = 3, C) in the micellar phase of FeSSIF*+SO (orange, solid line) and FeSSIF-V2 + SO media (dark blue, dashed line). For the total lipids, the theoretical concentration of lipids was indicated as a horizontal line.

its chemical composition, nanoaggregate size and zeta potential were determined.

3.1.2. Chemical composition, zeta potential and nanoaggregate size of the micellar phase

The micellar phase was additionally characterized based on lipid concentration, charge, and size to obtain complete information about the changes in the micellar phase depending on pH (Fig. 2).

The obtained results from the chemical analysis were in agreement with the conclusions from the optical observations (Fig. 2A): at low pH (4.5–5.5), the majority of the lipids (80 % for FeSSIF*+SO and 75 % for FeSSIF-V2 + SO) were removed in the form of a lipid phase by the centrifugation protocol used for the collection of the micellar phase. At pH = 6.0, lipid concentrations in the micellar phase increased significantly and reached a plateau at pH = 6.5, supporting the hypothesis that at higher pH, oleic acid was transferred from the lipid phase to the micellar phase due to ionization and conversion to oleate salts.

The change in oleic acid ionization could be expected to result in a change in the zeta-potential of the colloids. Indeed, the zeta potential decreased to more negative values at pH ≥ 6.5 (*viz*. the colloids became more charged) due to the presence of the negatively charged oleate molecules on the surface of the measured colloids (Fig. 2B).

A logical question, which can follow the above discussion, is related to the size and type of the colloids. The measured Z-average particle diameter showed aggregates with size in the range of 200–300 nm at pH = 4.5–6.0, which abruptly decreased to 25–50 nm at pH ≥ 6.5 (Fig. 2C). This switch in particle size is in agreement with the pK_a of oleic acid (Salentinig et al., 2010) and the results from both the microscope images and zeta-potential measurements: the increase of pH leads to oleic acid ionization, which triggers the transition of oleic acid from the lipid phase to oleate in the micellar phase. This is further supported by the distribution of nanoaggregates by volume (Supplementary Fig. S2): at pH ≤ 6 we observed small (25–50 nm) micelles and larger aggregates (vesicles or nanodroplets, 100–1000 nm), whereas only the single peak at 25–50 nm remained at pH ≥ 6.5. Cryo-TEM measurements, which were not performed in the current study, are required to unambiguously determined whether the larger nanoaggregates were vesicles, nanodroplets or both. However, the number of these larger aggregates in the micellar phase apparently was low, as demonstrated by the low concentration of lipids in the micellar phase determined by chemical analysis (Fig. 2A).

3.2. pH-solubility profiles in the SIF media

The next question is how the changes of colloidal structures in the media will affect the apparent drug solubility. Hence, the solubility of 13 uncharged drugs was evaluated across a pH range of 4.5–7.5 in four fed-state SIF. Generally, the two baseline media (FeSSIF* and FeSSIF-V2) did

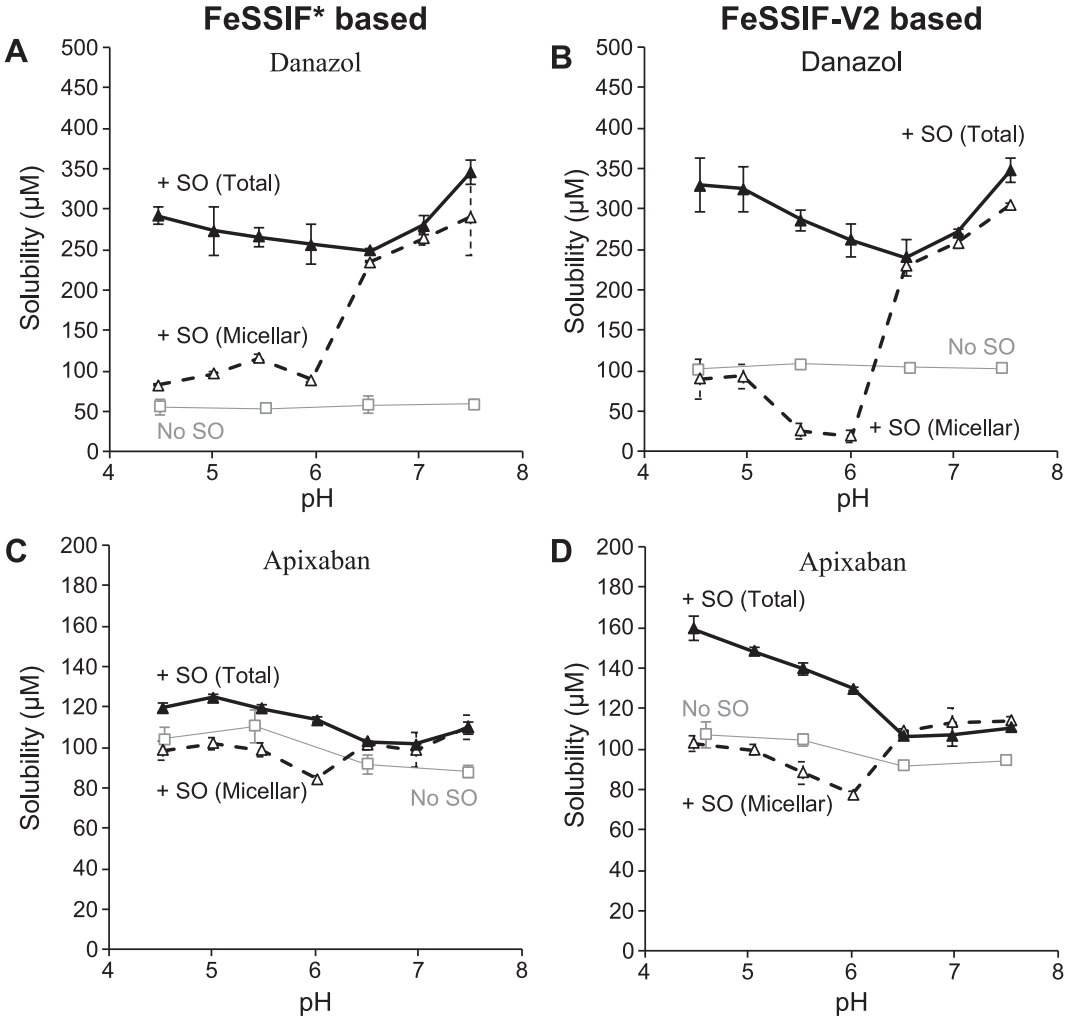

Fig. 3. pH-solubility profiles for representative compounds: danazol (A, B) and apixaban (C, D). No pH-dependent solubility was observed in the baseline media (No SO, grey line with square). Significant pH-dependent effects were observed in micellar phases (+ SO (Micellar), black dashed line with triangles) and total samples (+ SO (Total), black solid line with triangles) across both oleate-supplemented SIF media. All measurements were performed in triplicate (n = 3).

not cause significant pH-dependent solubility variations for any of the studied drugs, as illustrated for two representative compounds, danazol and apixaban (Fig. 3). In contrast, the oleate-supplemented SIF formed a lipid phase at low pH, which caused significant, pH-dependent differences between the solubilization capacity of the total sample (lipid + micellar) and the micellar phase for drugs like danazol (Fig. 3A and B), and smaller effects for compounds like apixaban (Fig. 3C and D). The pH vs. solubility profiles for the remaining 11 studied compounds are presented in Supporting Information (Supplementary Fig. S3).

The pH-solubility profiles of danazol and apixaban (Fig. 3) showed that both the indirect pH effect on solubility and the solubility range can vary considerably between compounds. To enable comparison across all 13 compounds, the ratios of micellar and total solubility in oleate-supplemented SIF media versus baseline media were analyzed in the following sections.

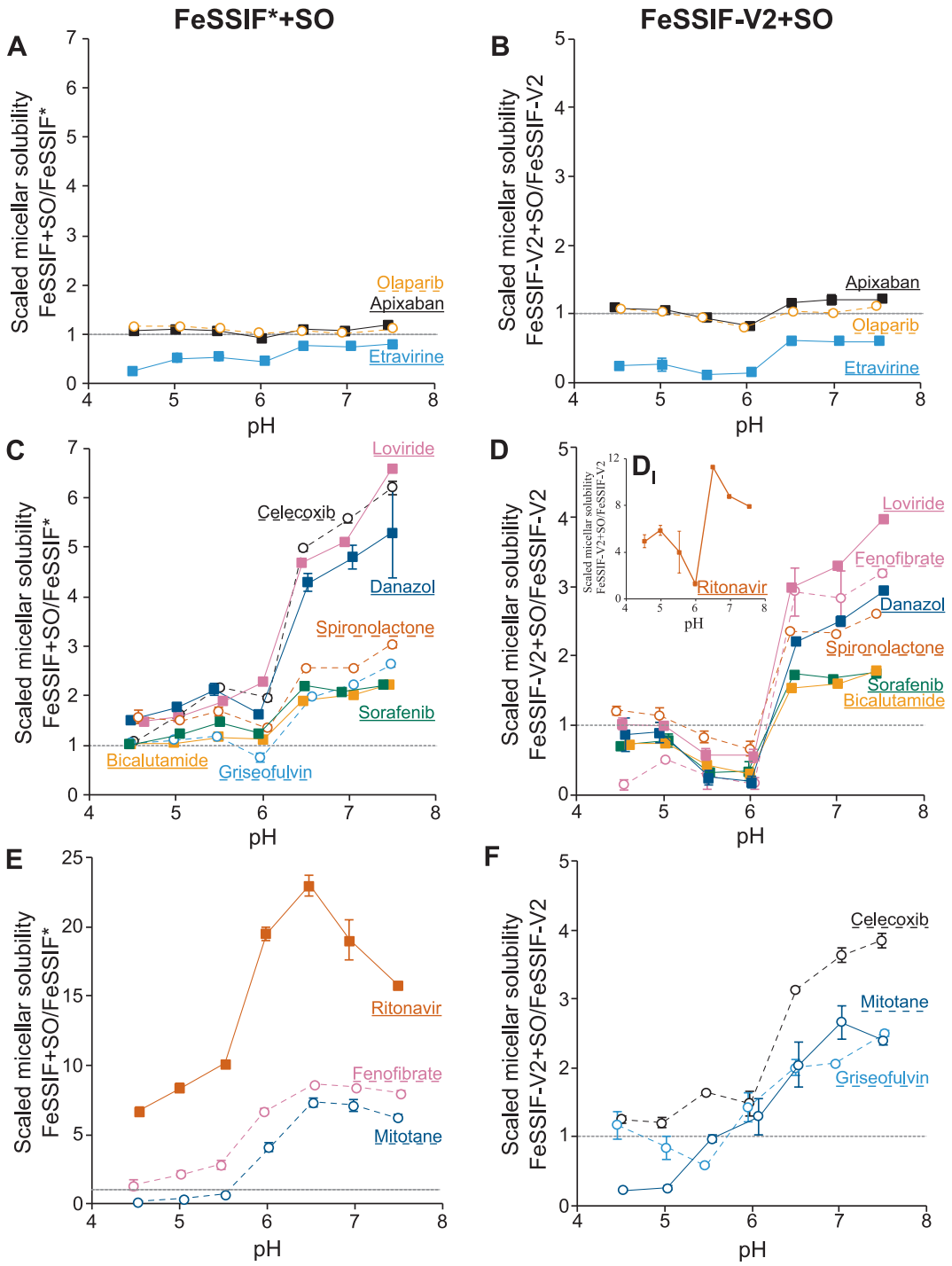

Fig. 4. Micellar solubility in FeSSIF*+sodium oleate and FeSSIF-V2 + sodium oleate, scaled with the FeSSIF* and FeSSIF-V2 solubility of each compound as a function of pH, for all compounds studied. Compounds were classified based on the shape of the pH-solubility profiles to enable comparison and separation of similarly behaving compounds. The dashed line at unity (y = 1) indicated that oleate did not affect drug solubility at the specific pH. Values below 1 indicated a decrease in micellar solubility relative to baseline, while values above 1 indicated an increase. All measurements were performed in triplicate (n = 3). All compounds shown in one graph using a logarithmic scale are presented in Supplementary Information Fig. S4.

3.3. Effect of sodium oleate on micellar solubility

The micellar solubility of all compounds studied in oleate-supplemented media was scaled with the respective baseline media (without oleate), Fig. 4. Oleate increased the solubility of 10 out of 13 compounds above baseline at pH > 6.0 (Fig. 4C–F) by forming (mixed) micelles which increased the solubilization capacity of the standard SIF media. The micellar solubility of three compounds (apixaban, olaparib, etravirine) showed minimal pH dependence regardless of the presence of monoolein (Fig. 4A and B).

While the micellar solubility of apixaban and olaparib was largely unaffected by oleate, etravirine showed a systematically lower micellar solubility in both oleate-containing media (Fig. 4A and B). The decreased solubility of etravirine at pH < 6 where a lipid phase is formed

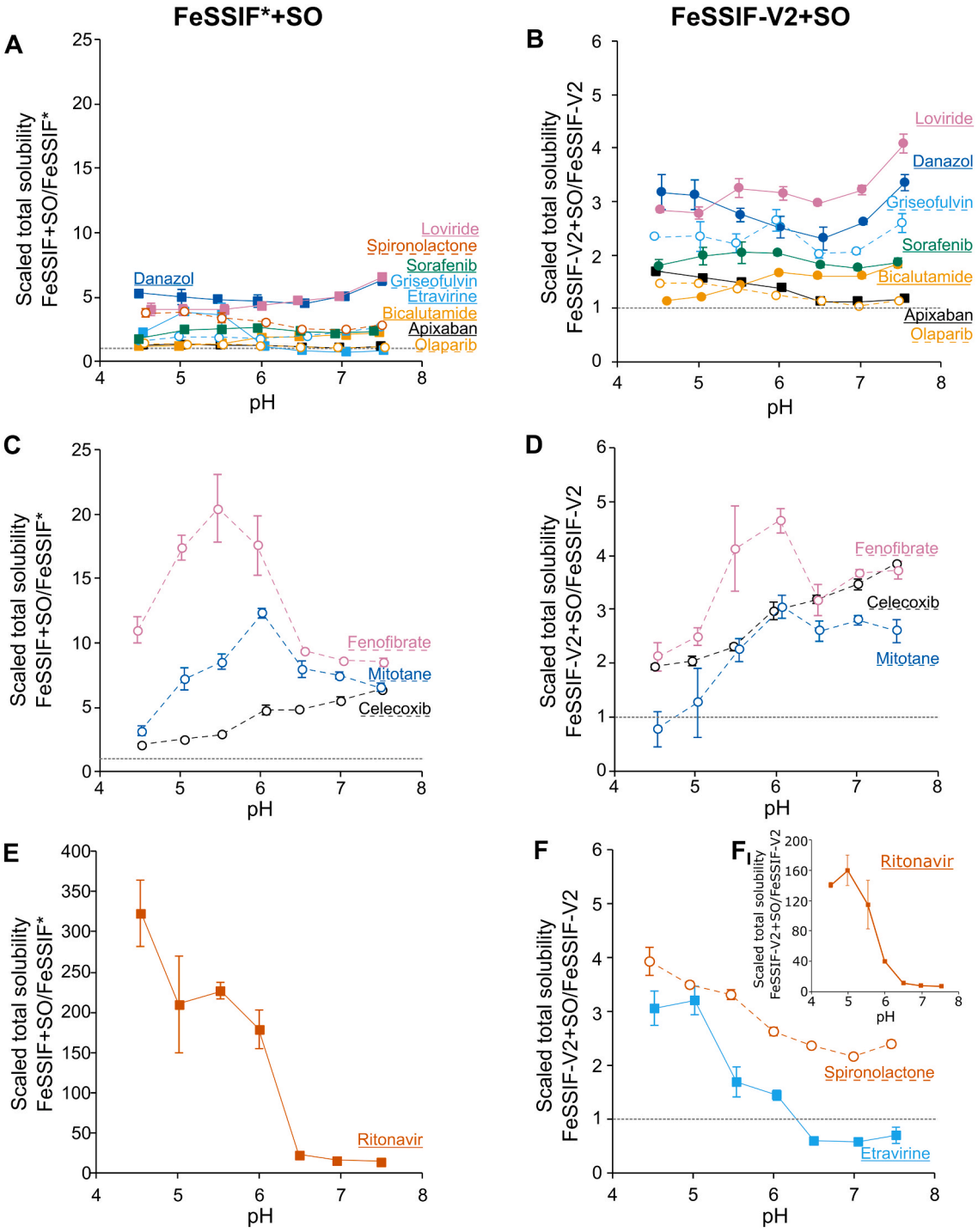

Fig. 5. Total solubility of all compounds as a function of pH, determined in FeSSIF*+sodium oleate and FeSSIF-V2 + sodium oleate. Solubility values were normalized to the average solubility in the corresponding baseline media (FeSSIF* and FeSSIF-V2). Compounds were classified based on the shape of the pH-solubility profiles to enable comparison and separation of similarly behaving compounds. Solubility in FeSSIF* and FeSSIF-V2 solubility does not depend on pH. The dashed line at unity (y = 1) means that oleate did not affect drug solubility at the specific pH. Values below 1 indicate a decrease in total solubility relative to baseline, while values above 1 indicate an increase. All measurements were performed in triplicate (n = 3). All compounds shown in one graph using a logarithmic scale are presented in Supplementary Information Fig. S4.

could be attributed to partitioning of the compound from the aqueous micellar phase to the lipid phase. Such effect of drug partitioning in the lipid phase may also explain the lower-than-baseline results for mitotane in both media at low pH. However, this hypothesis cannot explain the lower solubility of etravirine at high pH, where the lipid phase is absent (as it has been converted to micellar oleate), indicating a drug-specific, negative interaction between oleate and etravirine.

A more detailed examination of the shape of the pH-micellar solubility profiles for the 10 pH-dependent compounds showed additional effects (Fig. 4C–F). For both FeSSIF*+SO and FeSSIF-V2 + SO media, a dip in drug solubility was observed around pH = 6 for seven compounds (Fig. 4C and D). The effect was much more pronounced for the monoolein-containing media (FeSSIF-V2 + SO), where a significant negative effect (values below 1) and a clear minimum in solubility were observed at pH = 6 (Fig. 4D).

These observations (minimum in solubility) could be related to the centrifugation protocol used to obtain the micellar phase. The minimum in solubility at pH = 5.5 and 6.0 is most pronounced for the FeSSIF-V2 + SO media. In Fig. 1 we showed that a grainy structure, associated with nanodroplets was observed in the micellar phase at pH = 4.5 and 5.0, whereas a completely clear image was obtained at pH = 5.5 and 6.0. Similar results were obtained for FeSSIF*+SO. We could thus suggest that the observed minimum was not due to a factor which decreases the solubility at pH = 5.5 and 6.0, but to a factor which had instead increased the solubility at pH = 4.5 and 5.0: the presence of nanodroplets in the micellar phase.

One can also note that the set of compounds which did not exhibit a significant decrease in the micellar solubility around pH 6 was not the same for the FeSSIF*+SO and the FeSSIF-V2 + SO media. This may be explained by differences in the affinity of the compounds to the lipid phase which had a different composition depending on the presence of monoolein.

As an additional example of drug-specific behavior, ritonavir showed an exceptionally strong increase in the micellar solubility at high pH, compared to all other compounds: 25-fold in FeSSIF*+SO and 12-fold in FeSSIF-V2 + SO media (Fig. 4D$_I$ and E). Interestingly, the stronger increase in the micellar solubility for ritonavir existed over the full pH range compared to other compounds, which means that even a small amount of oleate in the micellar phase can affect micellar solubility for this compound. These results further indicate that while general trends can be consistent, drug-specific effects can lead to significant quantitative differences between compounds.

3.4. Effect of sodium oleate on the total solubility (micellar phase + lipid phase)

Similarly to the micellar solubility, the data for the total solubility was also analyzed after scaling to the baseline media (without oleate supplementation). In the case of FeSSIF*+SO, for 11 out of the 13 studied compounds, the addition of oleate increased the total solubility more than two-fold across most of the pH range studied (Fig. 5). Two compounds for which the solubility remained similar to baseline were those for which the micellar solubility was also not increased: apixaban and olaparib.

In contrast to FeSSIF*, which does not contain any monoglyceride, the monoolein in FeSSIF-V2 significantly increased the baseline solubility of the studied drugs (Fig. 3, Supplementary Fig. S3). This result aligns with previous studies, as monoglycerides have been shown to increase drug solubility (Katev et al., 2021; Kleberg et al., 2010; Porter et al., 2007). As a result, the number of compounds which displayed higher solubility than the baseline after the addition of oleate decreased to 9 out of 13 (Fig. 5B, D, and F). In addition to apixaban and olaparib, a negligible increase of total solubility was also measured for bicalutamide and sorafenib.

Regarding the effect of pH, the total solubility of 4 out of 13 compounds in the FeSSIF*+SO medium and 6 out of 13 compounds in the FeSSIF-V2 + SO medium exhibited significant pH dependence (Fig. 5C–F). Most of the compounds exhibiting pH-dependent total solubility were consistent across both media (fenofibrate, celecoxib, mitotane, and ritonavir), with spironolactone and etravirine showing a pH dependence only in FeSSIF-V2 + SO (Fig. 5F). Analysis of physicochemical properties suggested that compounds with pH-dependent total solubility tend to have a lower melting point than 160 °C (Table 1). An exception was etravirine, which also exhibited distinct behavior in micellar solubility (Fig. 4A and B).

The shapes of the pH-total solubility profiles varied among compounds (Fig. 5C–F). Celecoxib showed a continuous increase in solubility with increasing pH in both media (Fig. 5C and D), which could be explained by a higher affinity of this compound to micellar oleate, compared to the oleic acid in the lipid phase at lower pH. The other option is that the solubilization capacity for celecoxib of the smaller colloids is higher than that of the larger colloidal structures (Fig. 1).

The total solubility of fenofibrate and mitotane (Fig. 5C and D), which had the lowest melting point (<80 °C, Table 1), exhibited bell-shaped profiles as a function of pH, with a maximum around pH = 6 which suggested more complex phase distribution behavior around the pK_a of oleic acid.

In contrast, three compounds (ritonavir, spironolactone, etravirine) demonstrated a decrease in total solubility as pH increased (Fig. 5E and F). In this case, the results indicate that the drug partitioning in the oleic acid-based lipid phase at low pH was the main driver behind the high total solubility, whereas the affinity to the oleate mixed micelles obtained at high pH was lower. Hence, increasing pH decreased the amount of lipid phase due to the transition of oleic acid to oleate and its incorporation in the micelles, resulting in the observed decrease in total solubility with increasing pH. For the case of ritonavir, the exceptionally high drug concentrations measured at low pH in the total sample could be due to interactions of this weakly basic compound with oleic acid (Desai and Serajuddin, 2024).

3.5. Solubilization capacity of the lipid phase

The raw and scaled pH-solubility profiles presented in the previous sections showed that solubility behavior in total sample and micellar phase varied depending on the compound. To better understand the drug phase distribution between the lipid and micellar phase, solubility values were converted into the logarithm of the ratio between total and micellar solubility, log(tot/mic). This transformation sets the baseline at zero for samples for which there was no difference between total and micellar drug solubility and allowing an indirect assessment of compound partitioning.

For all media and all compounds studied, the total solubility exceeded the micellar solubility at pH values ≤6 (Fig. 6). In the FeSSIF*-based media, the total/micellar ratios of 5 out of 13 compounds (ritonavir, mitotane, etravirine, fenofibrate, and loviride) decreased slightly with the increase of pH from 4.5 to 5.5, then dropped near zero at pH ≥ 6.5 (Fig. 6A). For the other compounds, the ratio showed inconsistent behavior at pH 4.5 to 6.0: it either fluctuated around a constant value (sorafenib and olaparib) and then increased at pH = 6.0 (griseoflulvin, bicalutamide, and apixaban), or it decreased up to pH = 5.5 and then increased at pH 6.0 (danazol and celecoxib). In all cases, log(tot/mic) converged to zero at pH ≥ 6.5 due to the solubilization of the lipids (oleic acid) in the (mixed-)micelles in the form of oleate, which led to the disappearance of the lipid phase.

The total/micellar solubility ratio displayed more regular behavior in the FeSSIF-V2 media (Fig. 4B and D). Roughly half of the compounds (6 out of 13) showed a plateau in the low pH region (4.5–6.0), followed by a sharp decrease to zero at pH ≥ 6.5 (Fig. 4B). Four compounds (danazol, loviride, bicalutamide, sorafenib) showed an increase in the log(tot/mic) ratio with the increase of pH, which passed through a maximum around pH 5.5 to 6.0 (Fig. 6D), before decreasing to zero at pH ≥ 6.5. The last three compounds (fenofibrate, mitotane, and

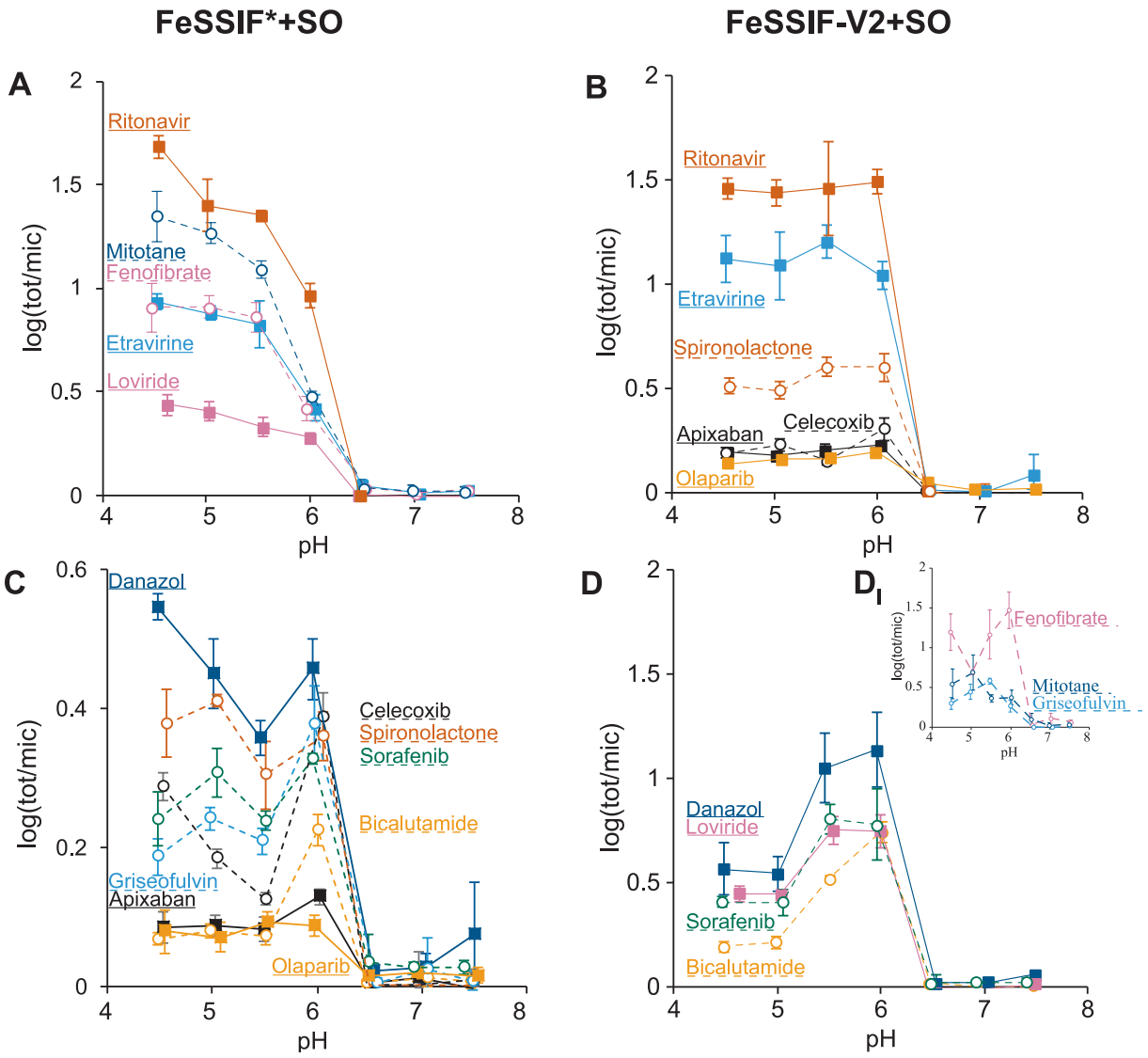

Fig. 6. Logarithm of the ratio between total and micellar solubility (log(tot/mic)) as a function of pH in the FeSSIF*+SO and the FeSSIF-V2 + SO media. A value equal to 0 indicates no difference between total and micellar solubility. Values above 0 indicated an increase in total solubility relative to micellar solubility.

griseofulvin) displayed inconsistent pH-dependent behavior (Fig. 6D$_I$). Fenofibrate showed a dependence similar to celecoxib and danazol in the FeSSIF*-based media, with the total/micellar solubility ratio initially decreasing with the increase of pH from 4.5 to 5.0, then increasing up to pH = 6.0, finally ending with an abrupt drop to zero at pH ≥ 6.5. Mitotane followed a similar trend to FeSSIF*: a gradually decreasing total/micellar solubility ratio up to pH = 6.0 and then dropping to zero at pH ≥ 6.5. For griseofulvin, the total/micellar solubility ratio increased up to pH 5.5 and then gradually decreased to zero at pH = 6.5.

All experimental results demonstrated that the indirect effect of pH on solubility depended on a compound-specific phase distribution between lipid and micellar phases. To clarify this structure–function relationship, the physicochemical properties of the studied drugs (Table 1) were assessed. The logarithm of the total/micellar solubility ratio at pH 5 was selected, as this pH either corresponds to the point of maximum effect for most compounds or represents a midpoint between increasing and decreasing log(tot/mic) trends. For FeSSIF*+SO, the best correlation ($R^2 = 0.85$) was obtained between the logarithm of the total/micellar solubility ratio at pH = 5.0 and $logP_{ow}$ (Fig. 7A), indicating that the impact of the indirect pH effect increased with the lipophilicity of the compounds. This finding is easily rationalized, considering that the mechanism of the indirect pH effect relates to compound partitioning in the lipid phase formed below pH = 6.

However, for FeSSIF-V2 + SO, the one-parameter correlation was weaker ($R^2 = 0.58$, Fig. 6B) compared to FeSSIF*+SO, and thus multi-parameter regressions with additional physicochemical parameters were explored. A two-parameter regression model, including $logP_{ow}$ and topological polar surface area (TPSA) as two independent variables, was obtained ($R^2 = 0.78$, Eq. (1), Fig. 7C). The two-parameter model indicated that more hydrophobic compounds with higher topological polar surface area had a stronger indirect pH effect at pH 5.

$$Log(tot/mic) = -0.5280 + 0.1991 \cdot logP_{ow} + 0.0036 \cdot TPSA \quad (1)$$

The above correlation indicates that when monoglycerides are present in the lipid phase, the polar groups of the compounds also play a role together with lipophilicity.

Based on the available limited dataset, it can be concluded that the indirect pH effect can affect the solubility of neutral drugs, and that the strength of the effect depends on drug lipophilicity and TPSA. However, it has to be noted that these conclusions are based on a relatively small dataset which limits extrapolation to compounds with significantly different chemical structure and physicochemical properties. Expanding the data would allow the definition of a more general and precise prediction model of the indirect effect of pH on solubility.

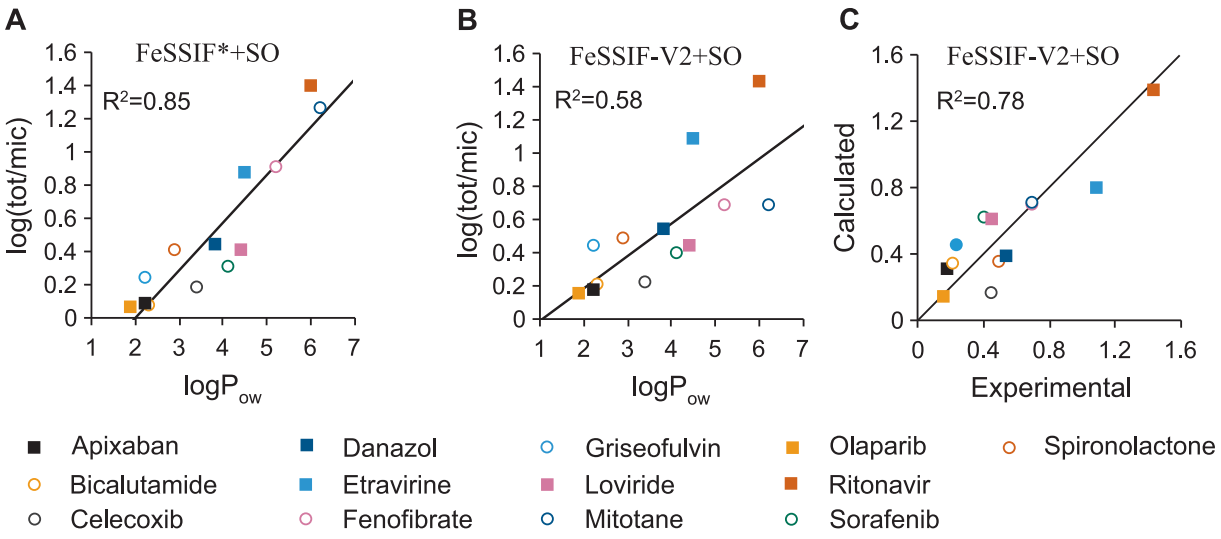

Fig. 7. Difference of solubilization capability in the total sample and micellar phase at different pH values represented as the logarithm of the ratio between total and micellar solubility (log(tot/mic)): one-parameter correlation with $logP_{ow}$ for FeSSIF*+SO media at pH 5 (**A**) and FeSSIF-V2 + SO media at pH 5 (**B**) and correlation between experimental and predicted values from two-parameter correlation (Eq. (1)) for FeSSIF-V2 + SO media at pH 5 (**C**). Points of varying colors and shapes represent specific compounds, as indicated in the legend.

3.6. Potential impact of the indirect pH effect to drug absorption

In the current work, we showed that SIF which have been enriched with a high concentration of sodium oleate to mimic fed state conditions can exhibit a strong indirect effect of pH on the apparent solubility of neutral compounds. This effect is caused by the pH-dependent transition between oleic acid and oleate (oleic acid $pK_a \approx 6.0$ in colloidal structures (Salentinig et al., 2010)) in the simulated intestinal fluids: at pH $\leq$ 6.0 a lipid phase (oleic acid droplets) drives the partitioning of lipophilic drugs, whereas at pH $\geq$ 6.5 the oleic acid converts to oleate and the lipid phase is solubilized in the intestinal bile salt and phospholipid micelles (Fig. 8). Hence, at low pH, the lipid phase increases the overall drug solubility in the total sample (lipid + micellar phase) but usually reduces the solubility in the micellar phase, indicating that the partitioning constant of lipophilic drugs between the lipid phase and the micelles is skewed towards the lipid phase. At pH $\geq$ 6.5, oleic acid is largely transferred to the micelles and there are no microscopic ($\geq$1 μm) lipid droplets left, resulting in no significant difference between micellar and total solubility. Thus, the indirect pH effect was explained by drug partitioning between the micellar and lipid phases, formed at these conditions.

From the viewpoint of the conditions observed in the human small intestine, the indirect pH effect occurs in a biorelevant pH window (Dahlgren et al., 2021; Harder et al., 2025; Riethorst et al., 2016b; Vinarov et al., 2021): a number of studies of aspirated human fed state intestinal fluids show median pH values varying between pH = 5.3 and 6.3. Moreover, the median duodenal pH can fluctuate widely depending on time point, ranging from 5.8 to 6.5 after the administration of a liquid meal and from 3.9 to 6.4 following the administration of an FDA breakfast (Harder et al., 2025). Very low duodenal pH values occur only briefly, but they may still influence drug behavior. If a drug dissolves more readily in large lipid droplets under these conditions, its

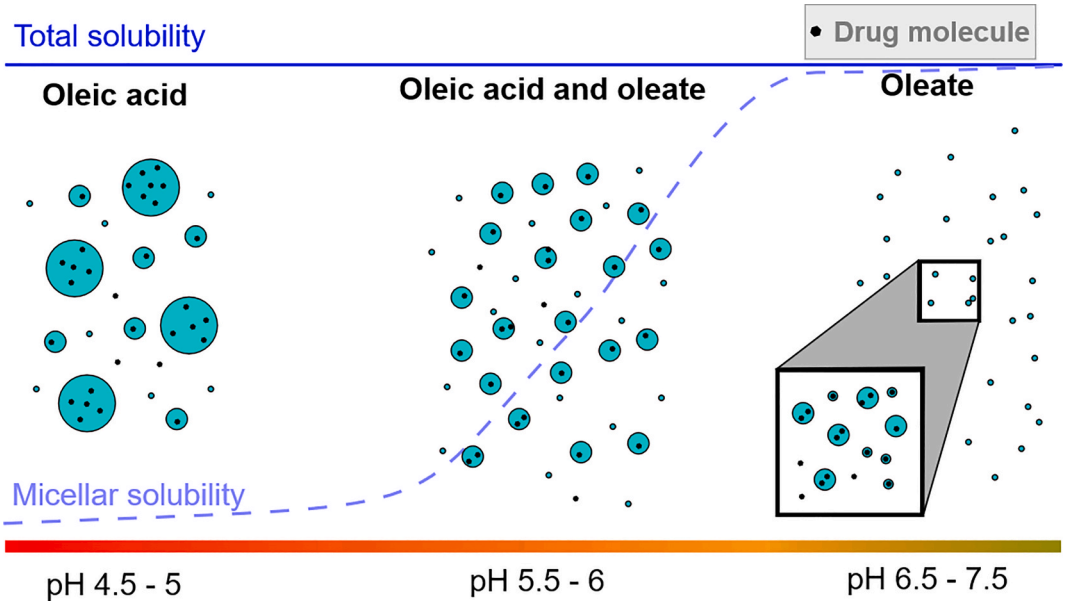

Fig. 8. Schematic diagram illustrating the indirect pH effect, showing changes in droplet size, transition between oleic acid (lipid droplets) and oleate (micelles), and solubility of the drug depending on pH.

absorption could be enhanced, a finding that requires further investigation. Importantly, the indirect pH effect may also play a role in the jejunum, where pH typically ranges from 5.0 to 8.0 (Harder et al., 2025). This broad pH range in both the duodenum and jejunum suggests that the formation of a lipid phase by the fatty acids produced during fat digestion could be expected *in vivo*, as well as the associated effect on the apparent drug solubility, which was described in the current study.

However, to predict in what direction the expected partitioning of a drug in the created lipid phase would affect drug absorption is more difficult. From one point of view, the lipid phase can act as a reservoir for drug, reducing its thermodynamic activity and thus the amount of free drug available for absorption – similarly to what has been reported for micellar solubilization (Amidon et al., 1982). However, it has to be kept in mind that although the concentration-normalized apparent permeability might decrease, the total permeated amount may still be higher compared to non-solubilized reference due to the concentration advantage (Amidon et al., 1982). Increased absorption of clofazimine and even increased apparent permeability has been shown for mixed bile salt and oleic or linoleic acid micelles in rats (O'Reilly et al., 1994). Furthermore, recent evidence shows that lipid droplets may also transport drug cargo across the enterocytes via endocytosis or paracellular pathways, although the contribution to overall absorption may be small (Debotton et al., 2022; Ghosh et al., 2023; Khatri and Shao, 2017; Satarifard et al., 2018).

The observed pH-dependent changes in solubility and colloidal structures suggest a potential influence on drug absorption, mediated by the drug partitioning in lipid droplets at pH < 6.5. This is supported by findings from lipid-based formulation studies, where absorption can be significantly increased compared to crystalline drug (Porter et al., 2007; Williams et al., 2013). To further confirm physiological relevance, studies using human intestinal fluids would be useful to confirm the observed partitioning effects, along with studies on the kinetics of colloidal structure formation, particularly the transition from droplets to micelles induced by pH changes. These insights will be critical for evaluating whether this phenomenon can be used in formulation development or reliably incorporated into in silico models predicting drug behavior under physiological conditions.

4. Conclusion

This study demonstrates that uncharged (neutral) drugs can exhibit pronounced pH-dependent solubility in SIF with added lipids, despite the absence of drug ionization. While reference SIF media showed no notable pH effects, oleate-supplemented media revealed substantial, compound-specific solubility changes driven by the transformation of colloidal structures. At pH 4.5–6.0, oleic acid formed lipid droplets that enhanced the solubility of lipophilic drugs in the total sample. When pH increased, oleic acid ionized and partitioned into the micellar phase, shifting the solubilization mechanism. This lipid-to-micelle transformation resulted in solubility differences up to 50-fold between total sample and micellar phase. Notably, at pH 5, the solubility ratio between total sample and micellar phase strongly correlated with drug lipophilicity or its combination with topological polar surface area ($R^2 \approx 0.8$). These findings highlight the importance of a deeper understanding of the interplay between pH, colloidal structures, and apparent solubility. The implementation of this knowledge will improve the predictive power of *in vitro* models used in oral drug development.

Declaration of Generative AI and AI-assisted technologies in the writing process

During the preparation of this work, M.O. used Grammarly and M365 Copilot in order to verify spelling, tone, and grammar. Afterwards, all authors reviewed and edited the content as needed and take full responsibility for the content of the published article.

CRediT authorship contribution statement

Mare Oja: Writing – review & editing, Writing – original draft, Visualization, Project administration, Methodology, Investigation, Funding acquisition, Formal analysis, Data curation, Conceptualization. **Sepanta Ehtemam:** Investigation. **Hristina Mircheva:** . **Brecht Goovaerts:** Methodology, Investigation. **Patrick Augustijns:** Writing – review & editing, Supervision, Resources, Project administration, Methodology, Funding acquisition, Conceptualization. **Zahari Vinarov:** Writing – review & editing, Supervision, Methodology, Conceptualization.

Declaration of competing interest

The authors declare the following financial interests/personal relationships which may be considered as potential competing interests: Mare Oja reports financial support was provided by European Union. Zahari Vinarov reports financial support was provided by Bulgarian National Science Fund. All other authors declare that they have no known competing financial interests or personal relationships that could have appeared to influence the work reported in this paper.

Acknowledgements

MO was supported by the European Union (grant agreement: 101108993). Views and opinions expressed are however those of the authors only and do not necessarily reflect those of the European Union or the European Research Executive Agency (REA). Neither the European Union nor the granting authority can be held responsible for them. ZV and HM acknowledge the support of the Bulgarian National Science Fund, National Research Program "VIHREN-2021", project 3D-GUT (№ KP-06-DV- 3/15.12.2021).

Appendix A. Supplementary data

Supplementary data to this article can be found online at https://doi.org/10.1016/j.ijpharm.2026.126647.

Data availability

The data supporting the findings of this study is available upon request.

References

Amidon, G.E., Higuchi, W.I., Ho, N.F.H., 1982. Theoretical and experimental studies of transport of micelle-solubilized solutes. J. Pharm. Sci. 71, 77–84. https://doi.org/10.1002/jps.2600710120.

Avdeef, A., 2007. Solubility of sparingly-soluble ionizable drugs. Adv. Drug Deliv. Rev. 59, 568–590. https://doi.org/10.1016/j.addr.2007.05.008.

Bauer, J., Spanton, S., Henry, R., Quick, J., Dziki, W., Porter, W., Morris, J., 2001. Ritonavir: an extraordinary example of conformational polymorphism. Pharm. Res. 18, 859–866. https://doi.org/10.1023/a:1011052932607.

Bioanalytical Method Validation Guidance for Industry | FDA [WWW Document], 2018. URL https://www.fda.gov/regulatory-information/search-fda-guidance-documents/bioanalytical-method-validation-guidance-industry (Accessed 9.01.2026).

Bou-Chacra, N., Melo, K.J.C., Morales, I.A.C., Stippler, E.S., Kesisoglou, F., Yazdanian, M., Löbenberg, R., 2017. Evolution of choice of solubility and dissolution media after two decades of biopharmaceutical classification system. AAPS J. 19, 989–1001. https://doi.org/10.1208/s12248-017-0085-5.

Cistola, D.P., Hamilton, J.A., Jackson, D., Small, D.M., 1988. Ionization and phase behavior of fatty acids in water: application of the Gibbs phase rule. Biochemistry 27, 1881–1888. https://doi.org/10.1021/bi00406a013.

Clarysse, S., Tack, J., Lammert, F., Duchateau, G., Reppas, C., Augustijns, P., 2009. Postprandial evolution in composition and characteristics of human duodenal fluids in different nutritional states. J. Pharm. Sci. 98, 1177–1192. https://doi.org/10.1002/jps.21502.

Dahlgren, D., Venczel, M., Ridoux, J.-P., Skjold, C., Mullertz, A., Holm, R., Augustijns, P., Hellstrom, P.M., Lennernas, H., 2021. Fasted and fed state human duodenal fluids: characterization, drug solubility, and comparison to simulated fluids and with human bioavailability. Eur. J. Pharm. Biopharm. 163, 240–251. https://doi.org/10.1016/j.ejpb.2021.04.005.

de Waal, T., Brouwers, J., Berben, P., Flanagan, T., Tack, J., Vandenberghe, W., Vanuytsel, T., Augustijns, P., 2023. Characterization of aspirated duodenal fluids from Parkinson's disease patients. Pharmaceutics 15, 1243. https://doi.org/10.3390/pharmaceutics15041243.

Debotton, N., Garsiani, S., Cohen, Y., Dahan, A., 2022. Enabling oral delivery of antiviral drugs: double emulsion carriers to improve the intestinal absorption of zanamivir. Int. J. Pharm. 629, 122392. https://doi.org/10.1016/j.ijpharm.2022.122392.

Desai, H.H., Serajuddin, T.M.A., 2024. Development of lipid-based SEDDS using digestion products of long-chain triglyceride for high drug solubility: formulation and dispersion testing. Int. J. Pharm. 654, 123953. https://doi.org/10.1016/j.ijpharm.2024.123953.

Dunn, C., Perrier, J., Khadra, I., Wilson, C.G., Halbert, G.W., 2019. Topography of simulated intestinal equilibrium solubility. Mol. Pharm. 16, 1890–1905. https://doi.org/10.1021/acs.molpharmaceut.8b01238.

Fagerberg, J.H., Bergström, C.A., 2015. Intestinal solubility and absorption of poorly water soluble compounds: predictions, challenges and solutions. Ther. Deliv. 6, 935–959. https://doi.org/10.4155/tde.15.45.

Ghosh, R., Satarifard, V., Lipowsky, R., 2023. Different pathways for engulfment and endocytosis of liquid droplets by nanovesicles. Nat. Commun. 14, 615. https://doi.org/10.1038/s41467-023-35847-z.

Goovaerts, B., Brouwers, J., Vinarov, Z., Braeckmans, M., Indulkar, A.S., Marmol, A.L., Borchardt, T.B., Tack, J., Koziolek, M., Augustijns, P., 2024. Understanding the impact of lipids on the solubilizing capacity of human intestinal fluids. Mol. Pharm. 21, 6398–6410. https://doi.org/10.1021/acs.molpharmaceut.4c00944.

Harder, F., Brouwers, J., Vanuytsel, T., Augustijns, P., 2025. Assessment of the dynamic nature of upper gastrointestinal pH: a pooled analysis using the fluid aspiration technique. Int. J. Pharm. 126377. https://doi.org/10.1016/j.ijpharm.2025.126377.

Jantratid, E., Janssen, N., Reppas, C., Dressman, J.B., 2008. Dissolution media simulating conditions in the proximal human gastrointestinal tract: an update. Pharm. Res. 25, 1663–1676. https://doi.org/10.1007/s11095-008-9569-4.

Katev, V., Vinarov, Z., Tcholakova, S., 2021. Mechanisms of drug solubilization by polar lipids in biorelevant media. Eur. J. Pharm. Sci. 159, 105733. https://doi.org/10.1016/j.ejps.2021.105733.

Khadra, I., Zhou, Z., Dunn, C., Wilson, C.G., Halbert, G., 2015. Statistical investigation of simulated intestinal fluid composition on the equilibrium solubility of biopharmaceutics classification system class II drugs. Eur. J. Pharm. Sci. 67, 65–75. https://doi.org/10.1016/j.ejps.2014.10.019.

Khatri, P., Shao, J., 2017. Transport of lipid nano-droplets through MDCK epithelial cell monolayer. Colloid. Surf. B Biointerf. 153, 237–243. https://doi.org/10.1016/j.colsurfb.2017.02.024.

Kim, S., Chen, J., Cheng, T., Gindulyte, A., He, J., He, S., Li, Q., Shoemaker, B.A., Thiessen, P.A., Yu, B., Zaslavsky, L., Zhang, J., Bolton, E.E., 2025. PubChem 2025 update. Nucl. Acids Res. 53, D1516–D1525. https://doi.org/10.1093/nar/gkae1059.

Kleberg, K., Jacobsen, J., Müllertz, A., 2010. Characterising the behaviour of poorly water soluble drugs in the intestine: application of biorelevant media for solubility, dissolution and transport studies. J. Pharm. Pharmacol. 62, 1656–1668. https://doi.org/10.1111/j.2042-7158.2010.01023.x.

Madsen, C.M., Feng, K.-I., Leithead, A., Canfield, N., Jorgensen, S.A., Mullertz, A., Rades, T., 2018. Effect of composition of simulated intestinal media on the solubility of poorly soluble compounds investigated by design of experiments. Eur. J. Pharm. Sci. 111, 311–319. https://doi.org/10.1016/j.ejps.2017.10.003.

O'Reilly, J.R., Corrigan, O.I., O'Driscoll, C.M., 1994. The effect of mixed micellar systems, bile salt/fatty acids, on the solubility and intestinal absorption of clofazimine (B663) in the anaesthetised rat. Int. J. Pharm. 109, 147–154. https://doi.org/10.1016/0378-5173(94)90142-2.

Porter, C.J.H., Trevaskis, N.L., Charman, W.N., 2007. Lipids and lipid-based formulations: optimizing the oral delivery of lipophilic drugs. Nat. Rev. Drug Discov. 6, 231–248. https://doi.org/10.1038/nrd2197.

Riethorst, D., Baatsen, P., Remijn, C., Mitra, A., Tack, J., Brouwers, J., Augustijns, P., 2016a. An in-depth view into human intestinal fluid colloids: intersubject variability in relation to composition. Mol. Pharm. 13, 3484–3493. https://doi.org/10.1021/acs.molpharmaceut.6b00496.

Riethorst, D., Mitra, A., Kesisoglou, F., Xu, W., Tack, J., Brouwers, J., Augustijns, P., 2018. Human intestinal fluid layer separation: the effect on colloidal structures & solubility of lipophilic compounds. Eur. J. Pharm. Biopharm. 129, 104–110. https://doi.org/10.1016/j.ejpb.2018.05.026.

Riethorst, D., Mols, R., Duchateau, G., Tack, J., Brouwers, J., Augustijns, P., 2016b. Characterization of human duodenal fluids in fasted and fed state conditions. J. Pharm. Sci. 105, 673–681. https://doi.org/10.1002/jps.24603.

Salentinig, S., Sagalowicz, L., Glatter, O., 2010. Self-assembled structures and pK_a value of oleic acid in systems of biological relevance. Langmuir 26, 11670–11679. https://doi.org/10.1021/la101012a.

Satarifard, V., Grafmüller, A., Lipowsky, R., 2018. Nanodroplets at membranes create tight-lipped membrane necks via negative line tension. ACS Nano 12, 12424–12435. https://doi.org/10.1021/acsnano.8b06634.

Schöller-Gyüre, M., Kakuda, T.N., Raoof, A., De Smedt, G., Hoetelmans, R.M.W., 2009. Clinical pharmacokinetics and pharmacodynamics of etravirine. Clin. Pharmacokinet. 48, 561–574. https://doi.org/10.2165/10895940-000000000-00000.

Suga, K., Kondo, D., Otsuka, Y., Okamoto, Y., Umakoshi, H., 2016. Characterization of aqueous oleic acid/oleate dispersions by fluorescent probes and Raman spectroscopy. Langmuir 32, 7606–7612. https://doi.org/10.1021/acs.langmuir.6b02257.

Suys, E.J.A., Warren, D.B., Porter, C.J.H., Benameur, H., Pouton, C.W., Chalmers, D.K., 2017. Computational models of the intestinal environment. 3. The impact of cholesterol content and pH on mixed micelle colloids. Mol. Pharm. 14, 3684–3697. https://doi.org/10.1021/acs.molpharmaceut.7b00446.

Van Eerdenbrugh, B., Froyen, L., Martens, J.A., Blaton, N., Augustijns, P., Brewster, M., Van den Mooter, G., 2007. Characterization of physico-chemical properties and pharmaceutical performance of sucrose co-freeze–dried solid nanoparticulate powders of the anti-HIV agent loviride prepared by media milling. Int. J. Pharm. 338, 198–206. https://doi.org/10.1016/j.ijpharm.2007.02.005.

Velozo, C.T., Cabral, L.M., Pinto, E.C., De Sousa, V.P., 2022. Lopinavir/ritonavir: a review of analytical methodologies for the drug substances, pharmaceutical formulations and biological matrices. Crit. Rev. Anal. Chem. 52, 1846–1862. https://doi.org/10.1080/10408347.2021.1920364.

Vertzoni, M., Alsenz, J., Augustijns, P., Bauer-Brandl, A., Bergström, C., Brouwers, J., Müllerz, A., Perlovich, G., Saal, C., Sugano, K., Reppas, C., 2022. UNGAP best practice for improving solubility data quality of orally administered drugs. Eur. J. Pharm. Sci. 168, 106043. https://doi.org/10.1016/j.ejps.2021.106043.

Vinarov, Z., Abdallah, M., Agundez, J.A.G., Allegaert, K., Basit, A.W., Braeckmans, M., Ceulemans, J., Corsetti, M., Griffin, B.T., Grimm, M., Keszthelyi, D., Koziolek, M., Madla, C.M., Matthys, C., McCoubrey, L.E., Mitra, A., Reppas, C., Stappaerts, J., Steenackers, N., Trevaskis, N.L., Vanuytsel, T., Vertzoni, M., Weitschies, W., Wilson, C., Augustijns, P., 2021. Impact of gastrointestinal tract variability on oral drug absorption and pharmacokinetics: an UNGAP review. Eur. J. Pharm. Sci. 162, 105812. https://doi.org/10.1016/j.ejps.2021.105812.

Vinarov, Z., Katev, V., Burdzhiev, N., Tcholakova, S., Denkov, N., 2018. Effect of surfactant–bile interactions on the solubility of hydrophobic drugs in biorelevant dissolution media. Mol. Pharm. 15, 5741–5753. https://doi.org/10.1021/acs.molpharmaceut.8b00884.

Weuts, I., Dycke, F.V., Voorspoels, J., Cort, S.D., Stokbroekx, S., Leemans, R., Brewster, M.E., Xu, D., Segmuller, B., Turner, Y.T.A., Roberts, C.J., Davies, M.C., Qi, S., Craig, D.Q.M., Reading, M., 2011. Physicochemical properties of the amorphous drug, cast films, and spray dried powders to predict formulation probability of success for solid dispersions: etravirine. J. Pharm. Sci. 100, 260–274. https://doi.org/10.1002/jps.22242.

Williams, H.D., Trevaskis, N.L., Yeap, Y.Y., Anby, M.U., Pouton, C.W., Porter, C.J.H., 2013. Lipid-based formulations and drug supersaturation: harnessing the unique benefits of the lipid digestion/absorption pathway. Pharm. Res. 30, 2976–2992. https://doi.org/10.1007/s11095-013-1126-0.